High-Photoluminescence-Yield Gold Nanocubes: For Cell Imaging and Photothermal Therapy

Xi Wu,[†] Tian Ming,[∥] Xin Wang,[‡] Peinan Wang,[§] Jianfang Wang,[∥,*] and Jiyao Chen[†,*]

[†]Surface Physics Laboratory (National Key Laboratory), Department of Physics, Fudan University, Shanghai 200433, China, [‡]Department of Microbiology and Microbial Engineering, School of Life Sciences, Fudan University, Shanghai 200433, China, [§]Department of Optical Science and Engineering, Fudan University, Shanghai 200433, China, and [∥]Department of Physics, the Chinese University of Hong Kong, Shatin, Hong Kong, China

ABSTRACT Gold nanocubes demonstrate unique optical properties of the high photoluminescence (PL) quantum yield and a remarkably enhanced extinction band at 544 nm. The 4×10^{-2} PL yield, which is about 200 times higher than that of gold nanorods, allows gold nanocubes to be successfully used in cell imaging of human liver cancer cells (QGY) and human embryo kidney cells (293T) with a common method of single-photon excitation. The high extinction coefficients of gold nanocubes also facilitate them carrying out the photothermal therapy of QGY and 293T cells, showing similar photokilling efficiency as compared to gold nanorods.

KEYWORDS: gold nanocubes · photoluminescence · cell imaging · photothermal therapy

Photoluminescence (PL) from bulk gold was first reported by Mooradian and later observed as a broad background in surface-enhanced Raman scattering.[1,2] It was found that the emission peak was centered near the interband absorption edge of the metal and therefore was attributed to the radiative recombination of the excited electrons in the sp band with the holes in the d band.[3−5] The PL quantum yield of bulk gold is as low as on the order of 10^{-10}.[1] Recently, the PL has been highly enhanced in gold particles with sizes ranging from 10 to 100 nm, due to the surface plasmon resonance (SPR)-involved local field enhancement.[6,7] Among nanoparticles with different structures, the gold nanorod has proven to be the most flexible structure owing to synthetic control of their sizes and aspect ratios.[8,9] Gold nanorods have two surface plasmon bands. The transverse one is at 520 nm, and the longitudinal band depends on the aspect ratio of rods.[4] With the increment of the aspect ratio, the intensity of the SPR longitudinal mode as well as the extinction band would be enhanced with the increased wavelength, such as at the infrared region of 750−850 nm for gold nanorods with the aspect ratio of ~4.[10,11] The strong SPR enhances the radiative rate of the electron−hole recombination in gold nanorods resulting in a considerable PL enhancement. Although the PL quantum yield is still not higher than 10^{-3},[10,12] the two-photon absorption cross section of gold nanorods reaches 2300 GM, much higher than that of organic fluorophores, providing a modality to detect these rods by means of two-photon excitation (TPE).[13] To obtain TPE images, the power density of the infrared femtosecond (fs) laser must be high enough to reach the threshold of two-photon absorption.[14] However, under the irradiation with such a high power density, gold particles could be melted because of the photothermal effect.[15] It was reported that a near-infrared fs laser (a few milliwatts) with an objective of 40× and 0.75 NA can melt gold particles,[16] and such a near-infrared fs laser with the low power of 0.25 mW already initiated the melting of gold nanorods by a 1.4 NA objective.[17] The rod melting caused a spectral shift of PL as well as a decrement of PL intensity.[17] Since the laser excitation with a milliwatt level was commonly used for TPE imaging in living systems,[18−20] the photothermal effects would thus influence the TPE detection of gold nanoparticles in biological systems.

Different from the TPE, there is no limitation on the power density for single-photon excitation (SPE), and the SPE is commonly used in biological imaging. However, if the fluorescence quantum yield of the probe is too low, like that of 10^{-4} for gold nanorods, the signals will be drowned by the interferences of native fluorophores in living systems. Therefore, developing gold nanoparticles with high PL quantum yields is probably a method for application of biological imaging with SPE.

*Address correspondence to jfwang@phy.cuhk.edu.hk, jychen@fudan.edu.cn.

Received for review August 24, 2009 and accepted December 08, 2009.

Published online December 16, 2009.
10.1021/nn901064m

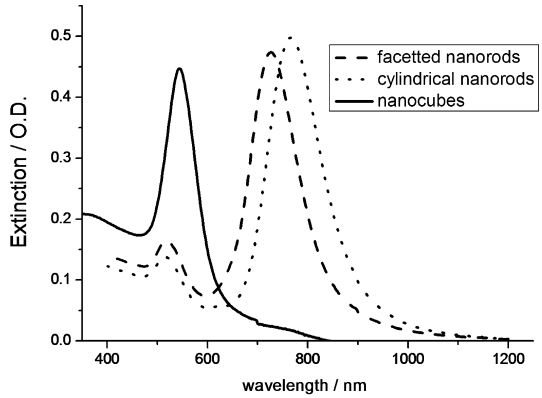

Figure 1. Extinction spectra of gold nanoparticles in aqueous solutions with a concentration of 0.1 nM.

It was suggested by Boyd *et al.* in 1986 that the local field enhancement plays a dominate role on PL increments in metals with rough surfaces.[6] Later, this theoretical model was applied to understand the PL enhancements in gold nanorods.[10,12] The origin of local field enhancements was summarized into two factors, the "lightning rod effect" (at a sharp angled surface) and localized SPR modes.[21] It has been found in gold nanorods with different aspect ratios that the PL becomes stronger when the longitudinal band of SPR is close to the region of interband transition, due to the mechanism where the PL is enhanced *via* coupling to localized SPR, and the PL would thus be enhanced more when the overlapping of the spectral regions between the SPR band and PL band is satisfied.[12] Therefore, if we can increase the lightning rod effect with more sharp tips or edges in gold nanoparticles and control the SPR band nearing the PL band in the mean time, the PL quantum yield might be dramatically increased. Among the gold nanoparticles with different structures, the gold nanocube seems to be a suitable candidate for satisfying these two conditions. The nanocubes have typical sharp edges, and they have a single SPR band which should be close to the region of interband transition and thus well overlap with the PL band. In this work, the gold nanocubes were selected to study their PL properties under SPE and TPE and compared with gold faceted nanorods and gold cylindrical nanorods. We found for the first time that the PL quantum yield of gold nanocubes reaches 4×10^{-2}, about 200 times higher than that of gold nanorods. Gold nanocubes demonstrated the versatile features not only for cell imaging with SPE but also for the photothermal therapy of cancer cells.

RESULTS AND DISCUSSION

Gold nanocubes, faceted nanorods, and cylindrical nanorods were prepared using a seeding growth method, as described previously.[22−28] The extinction spectra of these nanoparticles are shown in Figure 1, and their TEM images are shown in Figure 2. The faceted nanorods have a cuboid-like structure and thus were selected for comparison. The faceted nanorods also have typical transverse and longitudinal extinction bands, similar to those of cylindrical nanorods (Figure 1). Interestingly, the gold nanocubes have a remarkably enhanced extinction band with a center wavelength of 544 nm, as a small red shift can be found comparing to the transverse band (520 nm) of gold nanorods in Figure 1.

The PL quantum yields of these three gold nanostructures were comparatively studied by taking rhodamine B as a reference sample with the known fluorescence quantum yield. The normalized emission spectra of these four samples in aqueous solutions under SPE of 405 nm are shown in Figure 3A. These gold nanoparticles show similar broad-band PL spectra in the region of 500−600 nm, which are in agreement with previous reports.[6,7,10,12] It was reported that single gold nanorods have two PL bands of 530 and 650 nm, which are attributed to the recombination of the electron near the Fermi surface with the hole near the *L* and *X* symmetry points, respectively.[21] In our measurements, the nanoparticle solutions were measured. The PL spectral intensities should therefore be the sum of the PL from individual particles. Our spectral results confirm the PL band around 530 nm and demonstrate that only the *L* band around 530 nm is pronounced in both faceted nanorods and cylindrical nanorods under SPE. The gold nanocubes exhibit a very strong PL band around 530 nm. Taking rhodamine B as a standard reference with the fluorescence quantum yield of 0.7,[29] the PL quantum yields of these three gold nanoparticles

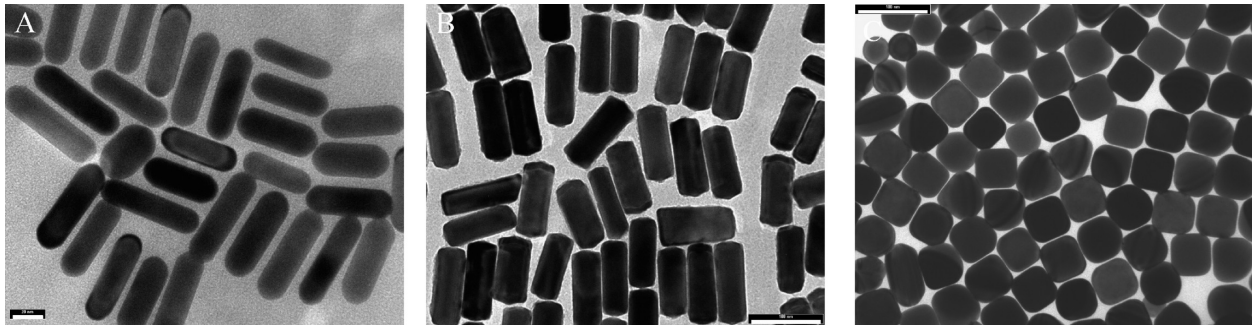

Figure 2. TEM images of (A) gold cylindrical nanorods with an aspect ratio of about 3.6; the bar is 20 nm. (B) Gold faceted nanorods with an aspect ratio of about 3.0; the bar is 100 nm. (c) Gold nanocubes with an edge length of about 45 nm; the bar is 100 nm.

TABLE 1. Optical Properties of Gold Nanoparticles

	gold cylindrical nanorods					
	this work	other works	gold faceted nanorods	gold nanocubes	gold nanosphere	gold nanocluster
PL yield (10^{-4})	1.9 ± 0.3	6[a] 1[b]	10 ± 1	420 ± 50	10^{-2} [c]	183 ± 32[d]
TPACS (GM)	2300[e]		65 ± 20	4.1 ± 1.5	—	—

[a]From ref 10. The aspect ratio of gold nanorods is 3.3. [b]From ref 12. The aspect ratio of gold nanorods is 3.25. [c]From ref 7. PL yields of gold nanospheres with the sizes from 6 to 30 nm are on the order of 10^{-6}. [d]From ref 30. Gold nanoclusters with the size about 2 nm. [e]From ref 13. TPACSs were measured at 800 nm.

were determined and are listed in Table 1. As predicted, the PL yield of nanocubes is 200 times higher than that of cylindrical nanorods, demonstrating that the local field enhancement can really increase the PL. The value (1.9×10^{-4}) of PL yield for cylindrical nanorods is very similar to the data of previous reports for gold nanorods with similar aspect ratios.[10,12] The PL yield of faceted nanorods is also obviously higher than that of cylindrical nanorods, attributed to the lightning rod effect, because there were more sharp edges in faceted nanorods than in cylindrical nanorods. However, the PL enhancement of faceted nanorods is still very weak compared to that of the nanocubes because of the worse overlapping of the SPR band and PL band for faceted nanorods, as seen in Figures 1 and 3A. Compared to the gold nanospheres with similar size, gold nanocubes particularly demonstrate the importance of lightning rod effect on PL enhancement. The PL quantum yield of gold nanospheres is reported to be not over 10^{-6},[7] due to their smooth surfaces.

The two-photon absorption cross sections (TPACSs) of these nanoparticles were comparatively measured by means of two-photon-induced fluorescence measurements. The PL spectra of the nanoparticle solutions under TPE of 800 nm fs laser are depicted in Figure 3B. Under TPE, the PL of nanocubes is very weak, but their PL spectrum of TPE is very similar to that of SPE with the PL peak of 530 nm. While for the faceted nanorods and cylindrical nanorods both *L* (530 nm) and *X* (650 nm) bands occur in the TPE PL spectra and two bands merge together, becoming a broadened band. Our spectral measurements were blocked around 650 nm due to the filter limitation of our system, but these TPE spectra are quite similar to previously reported TPE spectra of gold nanorods.[13] By comparing the TPE spectra with the SPE spectra, it can be seen that the 800 nm TPE produces the two PL bands for gold nanorods while the 405 nm SPE only favors the *L* band. The TPACSs of these nanoparticles at 800 nm are shown in Table 1. The TPACS of gold nanorods with an aspect ratio of 3.6 was reported to be 2300 GM. Taking the TPACS of gold cylindrical nanorods as the reference, the TPACSs of gold faceted nanorods and nanocubes are 37 times and 590 times smaller, respectively. These data are understandable, as Wang *et al.* have revealed that gold nanorods with the longitudinal SPR band near the excitation wavelength produce stronger PL than off-resonant gold nanoparticles.[13,30] Therefore, the cylindrical nanorods with the longitudinal SPR band of 766 nm have the highest TPACS, the faceted nanorods with the longitudinal SPR band of 726 nm have a relatively smaller TPACS value, and the nanocubes with the degenerate SPR band of 530 nm have the lowest value of TPACS.

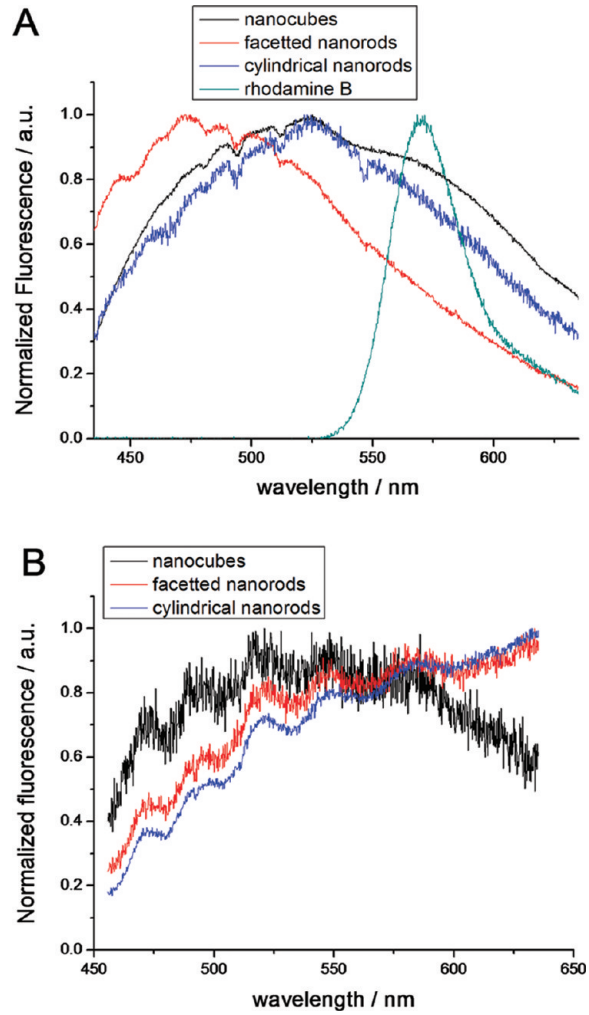

Figure 3. (A) Emission spectra of gold nanoparticle aqueous solutions and rhodamine B solution under SPE of 405 nm. (B) PL spectra of gold nanoparticle aqueous solutions under TPE of 800 nm.

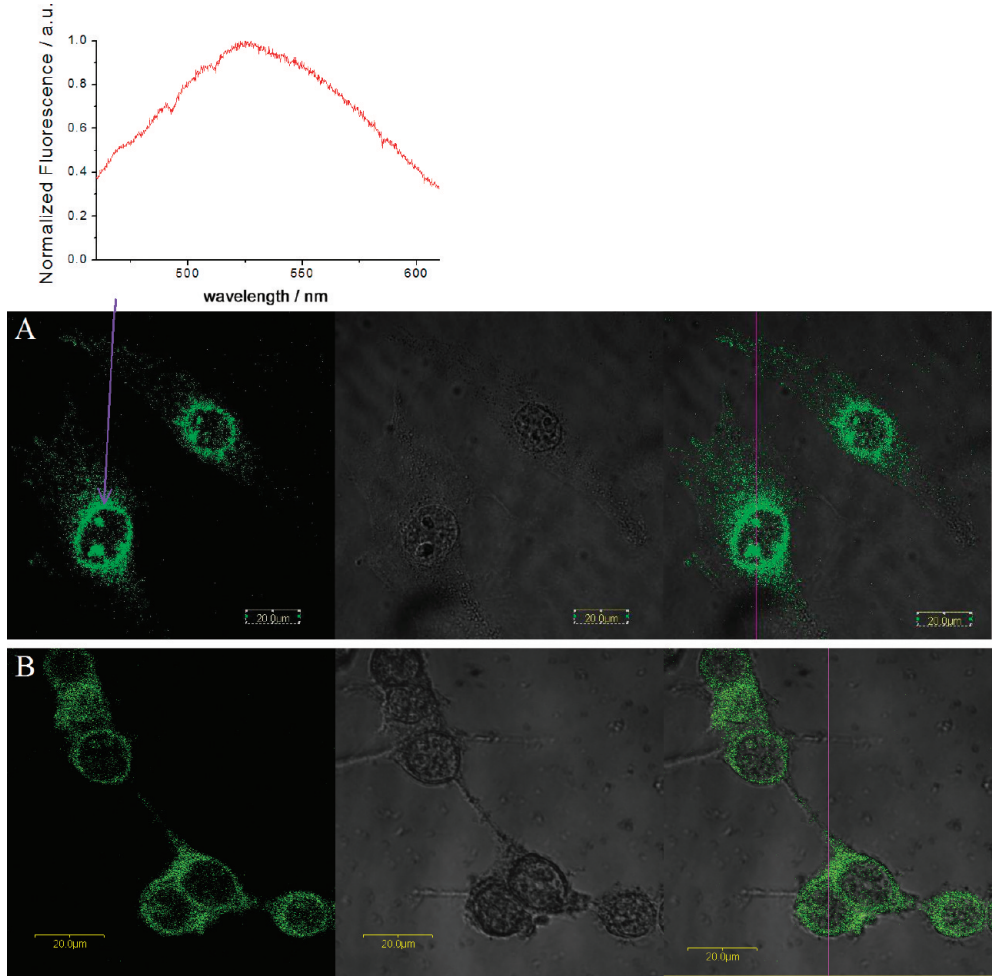

Figure 4. PL images of gold nanocubes in QGY cells (A) and 293T cells (B) with SPE of 488 nm. Detection channel: 505−550 nm. Left, PL image; middle, DIC image; right, merged image. Scale bar is 20 μm. The inset in image A shows the PL spectrum of cellular gold nanocubes at the spot indicated by the arrow.

The TPACS of gold nanocubes is so low that these nanocubes are not suitable for TPE imaging with near-infrared lasers in biological systems. However, the PL quantum yield of gold nanocubes is so high (0.042) (Table 1) that these nanocubes can be used for SPE imaging in living systems. We tested the ability of gold nanocubes for cell imaging with SPE in cell lines of QGY (human liver cancer cell) and 293T (human embryo kidney cell). After 1 h incubation with a particle concentration of 0.03 nM, nanocubes can be clearly seen in the cytoplasm of cells by means of confocal microscope with the 488 nm excitation for both QGY and 293T cells (Figure 4). Herein, the 488 nm laser was selected for the excitation because the relatively low autofluorescence of native fluorophores in cells at this excitation wavelength is induced as compared with the excitation of the shorter wavelength. The advantages of the high PL quantum yield and the remarkable cellular uptake rate, as shown in Figure 4, demonstrate that gold nanocubes have the potential to be used in cell imaging with common SPE. Recently, Lin *et al.* prepared small gold nanoclusters (AuNC@DHLA, 2 nm in size) with the PL yield of 0.018 in water and found that these gold nanoclusters can be used as the fluorescence dye to stain cells.[30] Therefore, the gold nanoparticles with the high PL yield have the potential to be used for cell imaging and biological labeling.

When cells have been incubated with gold nanorods at the same concentration as that of gold nanocubes, no detectable PL images with SPE in the same confocal microscope could be found due to the extremely low PL quantum yield of nanorods. The PL images of cellular gold cylindrical nanorods can be recorded with TPE of 800 nm fs laser in both QGY and 293T cells because of the high TPACS of nanorods (Figure 5), in agreement with previous reports on other cell lines.[14,18,19,31] However, to acquire TPE images, the power of the fs laser was about 1 mW, which is much higher than the power of 50 μW of the continuous wave (CW) 488 nm laser used for measuring SPE images.

As shown in Figure 1, the extinction coefficients of the 544 nm band of gold nanocubes are almost the same as that of nanorods at the 766 nm band. On the basis of the high light absorption of the longitudinal ex-

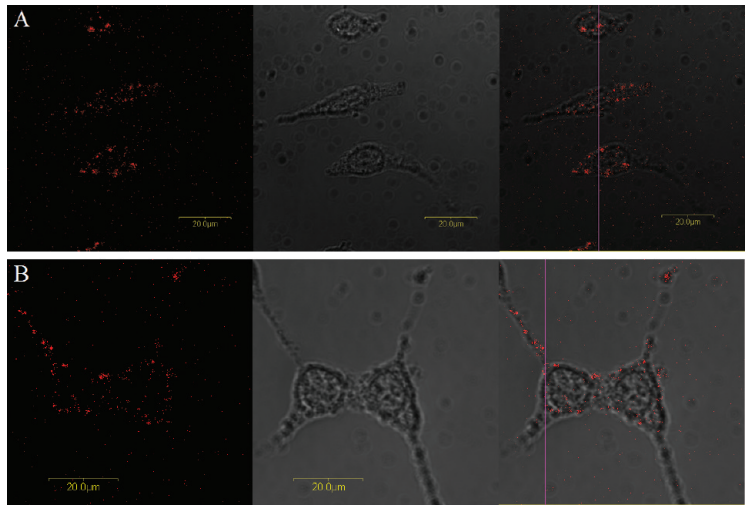

Figure 5. PL images of gold cylindrical nanorods in QGY cells (A) and 293T cells (B) under TPE of 800 nm. Detection channel: 580−640 nm. Left, PL image; middle, DIC image; right, merged image. The scale bar is 20 μm.

tinction band, gold nanorods have been successfully used in photothermal therapy of cancer cells with infrared lasers. Herein, the 532 nm CW laser, located in the region of the 544 nm extinction band of nanocubes, was used to test the photothermal effect of gold nanocubes on QGY and 293T cells. As shown in Figure 6A, after nanocube incubation with a final particle concentration of 0.01 nM and the 532 nm irradiation with a power density of 4 W/cm^2 for 15 min, most QGY cells were dead as the PI-positive signals were clearly seen. In contrast, the nanocube-loaded cells without the laser irradiation did not show any PI-positive signals (Figure 6B), demonstrating that the gold nanocubes alone did not cause the detectable damage to cells. When control cells (without nanocube treatments) were irradiated with the same dose, no cell damaging was detected also. Similar results were seen in 293T cells, where the photothermal effect of cellular nanocubes destroyed cells, while nanocubes alone (without irradiation) had negligible damage on cells (Figure 6C,D). These results suggest that gold nanocubes also can be used in photothermal therapy of cancer cells. Although gold nanocubes can carry out photothermal therapy for cancer cells with the irradiation of visible light, they have no absorption band in the near-IR region, and thus these nanocubes are not as useful as gold nanorods for photothermal therapy because the near-IR region is the light tissue window.

For comparison, the photothermal therapies of gold nanorods on QGY and 293T cells were carried out in parallel. The incubation concentration of nanorods was 0.01 nM, the same as that of nanocubes, and an irradiation power density of the 800 nm fs laser was also 4 W/cm^2 with an irradiation time of 15 min. The PI-positive signals in Figure 7 demonstrate that both QGY and 293T cells were damaged after irradiation, but no obvious PI signals were observed in nanorod-loaded cells without irradiation. In this experiment, the unfocused laser beams were used to carry out the *in vitro* photother-

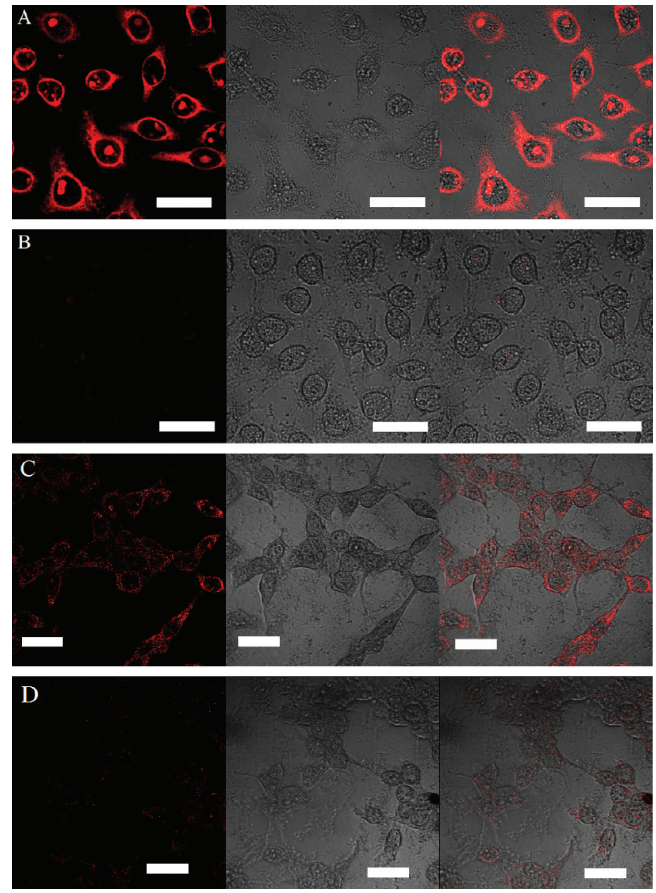

Figure 6. Cell damaging detection with PI in nanocube-loaded cells. PI detection was in 580−640 m channel, excited by 488 nm laser. (A) Nanocube-loaded QGY cells have been irradiated by the 532 nm laser for 15 min with a power density of 4 W/cm^2. (B) Nanocube-loaded QGY cells without irradiation. (C) Nanocube-loaded 293T cells have been irradiated by the 532 nm laser for 15 min with a power density of 4 W/cm^2. (D) Nanocube-loaded 293T cells without irradiation. Left, PI fluorescence image; middle, DIC image; right, merged image. Scale bar is 30 μm.

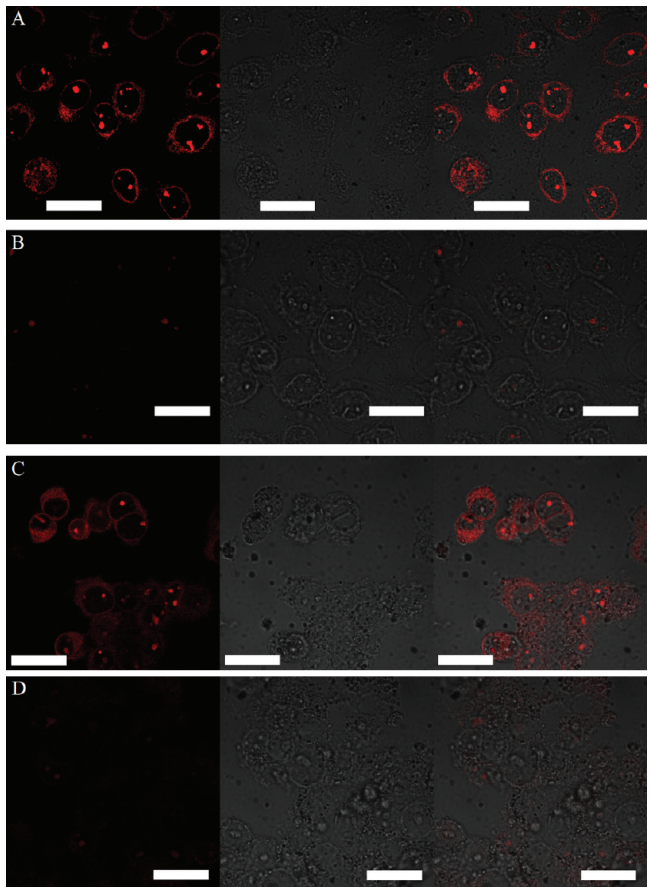

Figure 7. Cell damaging detection with PI in nanorod-loaded cells. PI detection was in the 580−640 nm channel, excited by the 488 nm laser. (A) Nanorod-loaded QGY cells have been irradiated by the 800 nm laser for 15 min with a power density of 4 W/cm^2. (B) Nanorod-loaded QGY cells without irradiation. (C) Nanorod-loaded 293T cells have been irradiated by the 800 nm laser for 15 min with a power density of 4 W/cm^2. (D) Nanorod-loaded 293T cells without irradiation. Left, PI fluorescence image; middle, DIC image; right, merged image. The scale bar is 30 μm.

mal therapy. We found that an irradiation density of 4 W/cm^2 and irradiation time of 15 min can thoroughly damage QGY and 293T cells. Huang *et al.* found that the threshold for the photothermal killing of two malignant epithelial cell lines (HOC and HSC) with gold nanorods is 10 W/cm^2 with 4 min.[32] Hauck *et al.* reported that the serious damaging of OCI leukemia cells and MCF-7 breast cancer cells with gold nanorods required 2 W/cm^2 light for 30 min.[33] Although the cell lines are different, it seems that the light dose level is similar for the photothermal therapy with gold nanorods. However, Skrabalak *et al.* reported that the damaging of SK-BR-3 cells with gold nanocages only required 1.5 W/cm^2 light for 5 min,[34] and Li *et al.* found recently that circularly polarized light is more efficient in gold nanorod-mediated cancer photothermal therapy with much lower power densities.[31]

CONCLUSIONS

In summary, gold nanocubes exhibit the highest PL quantum yield among gold nanoparticles with different structures, probably due to the particularly local field enhancement including the effects of "lightning rod effect" and enhanced SPR band at the region well overlapped with the PL band. The *in vitro* works suggest that gold nanocubes can be used as fluorescence probes for cell imaging with common SPE. In addition, gold nanocubes also can carry out the photothermal therapy of cancer cells using visible light with an efficiency similar to that of gold nanorods. Therefore, gold nanocubes are versatile nanoparticles and worth further investigation for biological applications.

METHODS

Preparation of Gold Nanoparticles. Gold nanorods were prepared using a seeding growth method as described previously.[22,28] As-prepared nanorods were stabilized by cetyltrimethylammonium bromide (CTAB) to form CTAB-coated gold nanoparticles. The obtained particle concentration was about 0.1 nM. Gold nanocubes were grown following a method report previously.[26] Specifically, the seeds were prepared by the addition of a freshly prepared, ice-cold aqueous $NaBH_4$ solution (0.01 M, 0.6 mL) into an aqueous mixture solution composed of $HAuCl_4$ (0.01 M, 0.25 mL) and CTAB (0.1 M, 7.5 mL), followed by rapid inversion mixing for 2 min. The resultant seed solution was kept at room temperature for 1 h before use. The growth solution was prepared by the sequential addition of CTAB (0.1 M, 6.4 mL), $HAuCl_4$ (0.01 M, 0.8 mL), and ascorbic acid (0.1 M, 3.8 mL) into water (32 mL). The CTAB-stabilized seed solution was diluted 10 times with water. The diluted seed solution (0.02 mL) was then added into the growth solution. The resultant mixture solution was mixed by gentle inversion for 10 s and then left undisturbed overnight. The average edge length of the as-prepared Au nanocubes is 45 ± 3 nm.

Transmission electron microscopy (TEM) imaging was carried out on a FEI CM 120 microscope working at 120 kV, to measure the sizes of gold nanoparticles.

Cell Culture and Cell Treatments with Gold Nanoparticles. The QGY (human liver cancer cell) and 293T (human embryo kidney cell) cells were procured from the Cell Bank of Shanghai Science Academy. Cells were incubated in Dulbecco's modified Eagle's medium (DMEM) with Earle's salts containing 15% fetal bovine serum, 2% L-glutamine (all from Gibco), in an incubator with a humidified atmosphere (5% CO_2) at 37 °C. Cells in exponential phase of growth were used in experiments.

In cell imaging experiments, nanocubes or nanorods were added into the cell dishes with a final concentration of 0.03 nM. After incubation in the incubator for 1−2 h, cells were washed with PBS three times to remove unassociated nanoparticles and then added with the fresh culture medium. These cell samples were then ready for imaging measurements. Hauck *et al.* reported that the region of 0.02−0.1 nM incubation concentrations of CTAB-coated gold nanorods is safe for HeLa cells.[33] Therefore, the 0.03 nM incubation concentration of gold nanoparticles for cells was selected here.

In photothermal therapy experiments, cells in solutions were added with nanocubes or nanorods with a final concentration of 0.01 nM and then incubated for 1 h in an incubator. After removing unassociated nanoparticles, cells were irradiated by the 532 nm CW laser (Photop Suwtech, DTGL-3010) or 800 nm fs laser (Coherent, Mira 900-B) accordingly with an illumination area of about 3 mm^2. We adjusted the laser power to be around 120

mW, which was measured by a laser power meter (Coherent, FieldMaster), to make the irradiation power density of 4 W/cm^2 on cells for both irradiations of 532 and 800 nm. Control cells (without gold nanoparticle treatments) were also irradiated under the same conditions, respectively. Then, the 20 μL 0.1% propidium iodide (PI), a fluorescence dye commonly used to test the integrity of cell membranes, was added to each cell dish for 15 min. Finally, the damaged cells were evaluated as the PI-positive fluorescence signals occurred in the images of the fluorescence microscope.

Imaging and Spectral Measurements of Gold Nanoparticles with SPE and TPE. The PL images of cellular gold nanoparticles were acquired by a laser scanning confocal microscope (LSCM) (Olympus FV300, IX71) in detection channel 1 with a 505−550 nm band-pass filter. Differential interference contrast (DIC) images were recorded simultaneously in a transmission channel to exhibit the cell morphology. A water immersion objective (UplanApo, 60×, 1.2 NA) and a matched pinhole were used in experiments. Two beams of lasers were coupled into the LSCM as the excitation lines: 488 nm (Melles Griot, argon ion) for acquiring the SPE imaging and 800 nm femtosecond (fs) Ti:sapphire laser (Coherent, Mira 900-B) with 200 fs pulse width and 78 MHz reputation rate for acquiring the TPE imaging. The excitation light powers on the cell were about 50 μW for the 488 nm laser and about 1 mW for the 800 nm fs laser, measured by a power meter (Coherent, lasercheck). The PI-stained cells were also imaged in this LSCM but in another detection channel (channel 2) with a band-pass filter of 585−640 nm to collect the PI fluorescence centered at 630 nm. Since the fluorescence quantum yield of PI is about 10 times higher than that of gold nanocubes, the PL from gold nanoparticles did not cause a remarkable interference for the detection of PI signals.

On the basis of the obtained PL images, some parts of individual cells were chosen to measure microregion fluorescence spectra of cellular gold nanoparticles using the laser point-stay mode of the LSCM system. This mode allows the laser to stop scanning and continuously irradiate the selected spot for performing spectral measurements. A 405 nm laser (Coherent, Radius 405-25) was introduced into the LSCM as the excitation. The spectra were measured using a spectrometer (Acton, Spectropro 2150i) equipped with a liquid-nitrogen-cooled CCD (Princeton, Spec-10:100B LN). The PL output from the side exit of the microscopic system was directly focused onto the entrance slit of the spectrometer. However, due to the limitation of the dichroic mirror in the system, the microregion spectral measurement can be carried out for 405 and 800 nm lasers but not for 488 nm. The PL spectra of gold nanoparticles in solutions were also measured in this microscope system by using the solution sample sandwiched in a pair of coverslips instead of the cell dish. The microscope system is suitable for measuring the fluorescence from high scattering particles because the objective of 60× used in the system can ensure that the excitation of nanoparticles occurs in the shallow layer of the solution sample, which decreases the influence of the particle scattering in the optical path.

The PL Quantum Yield Measurements of Gold Nanoparticles. The PL quantum yields of gold nanoparticles were determined by a comparison method of the fluorescence emission with the standard reference sample of rhodamine B in solutions. Basically, the fluorescence emission of a sample can be written in a formula with related parameters.[35]

$$F = K\Phi c\sigma I l$$

where Φ is the fluorescence quantum yield of the sample, c is the fluorophores number density (concentration of the sample), σ is the one-photon absorption cross section, l is the length of the path in which photons are absorbed, I is the flux of incident photons (photons/cm^2 s), F is the integrated fluorescence signal in the emission region, and K is a parameter constant of the instrument. By measuring the emission spectra as shown in Figure 3A, the F_s (nanoparticle sample) and F_r (rhodamine B), corresponding to the emission regions in Figure 3A, respectively, were obtained. Here, all fluorescence signals were measured under SPE of 405 nm with the same experimental conditions in the same system, so that the K, I, and l are the same for nanoparticle samples and reference samples. Using the above formula for nanoparticles and rhodamine B, respectively, the PL quantum yield Φ_s of gold nanoparticles can then be determined by comparing with the known Φ_r of rhodamine B as follows:

$$\Phi_s = \frac{F_s}{c\sigma} \times \frac{c_r\sigma_r}{F_r} \times \Phi_r$$

where the term with a suffix r means the term for rhodamine B. Since the $c\sigma$ represents the absorption of the sample, the term of $c_r\sigma_r/c\sigma$ can be replaced by A_r/A_s. The A is the absorption coefficient of the sample at the excitation wavelength. Then the formula turns to the simple form.

$$\Phi_s = \frac{F_s}{A_s} \times \frac{A_r}{F_r} \times \Phi_r$$

When the values of A_r and A_s were measured, the Φ_s of nanoparticles can be obtained. Herein, we measured A_r and A_s, the absorption coefficients of the reference sample and nanoparticle sample, at the excitation wavelength of 405 nm in a spectrometer (HITACHI U-500) and then determined the Φ_s according to the formula.

Two-Photon Absorption Cross Section Measurements of Gold Nanoparticles. Similarly, the TPACSs of gold nanocubes and faceted nanorods were measured by comparing the TPE-induced PL with that of gold cylindrical nanorods. The relationship of the nanoparticle PL with related parameters under TPE is included in the following formula.[35]

$$F = K\Phi c l \delta I^2/2$$

where δ is the two-photon absorption cross section, I is the flux of incident photons, Φ is the PL quantum yield, and the F is the integrated PL of the sample under TPE. Since the TPACSs of gold cylindrical nanorods have been determined as 2300 GM,[13] the gold cylindrical nanorod sample was taken as the reference sample with the known δ_r for comparison. When the F values for gold nanocubes, faceted nanorods, and cylindrical nanorod were measured, the δ of the sample can be written in the δ_r related form and determined accordingly.

$$\delta = \frac{F}{F_r} \times \frac{\Phi_r c_r}{\Phi c} \cdot \delta_r$$

Acknowledgment. This work was supported by the Shanghai Municipal Science and Technology Commission (06ZR14005), the National Natural Science Foundation of China (10774027).

REFERENCES AND NOTES

1. Mooradian, A. Photoluminescence of Metals. *Phys. Rev. Lett.* **1969**, *22*, 185–187.
2. Heritage, P.; Bergman, J. G.; Pinczuk, A.; Worlock, J. M. Picosecond Raman Gain Spectroscopy of a Monolayer of Cyanide on Silver. *Chem. Phys. Lett.* **1979**, *67*, 229–232.
3. Plekhanov, V. G.; Siliukova, T. V. Experimental Manifestation of the d-Band Structure in the Photoluminescence Spectra of Gold. *Sov. Phys. Solid State* **1990**, *32*, 1268–1274.
4. Link, S.; El-Sayed, M. A. Size and Temperature Dependence of the Plasmon Absorption of Colloidal Gold Nanoparticles. *J. Phys. Chem. B* **1999**, *103*, 4212–4217.
5. Noginov, M. A.; Zhu, G.; Gavrilenko, V. I. Sensitized Nonlinear Emission of Gold Nanoparticles. *Opt. Express* **2007**, *15*, 15648–15655.
6. Boyd, G. T.; Yu, Z. H.; Shen, Y. R. Photoinduced Luminescence from the Noble Metals and Its Enhancement on Roughened Surfaces. *Phys. Rev. B* **1986**, *33*, 7923–7936.
7. Dulkeith, E.; Niedereichholz, T.; Klar, T. A.; Feldmann, J.; von Plessen, G.; Gittins, D. I.; Mayya, K. S.; Caruso, F. Plasmon Emission in Photoexcited Gold Nanoparticles. *Phys. Rev. B* **2004**, *70*, 205424.

8. Kelly, K. L.; Coronado, E.; Zhao, L. L.; Schatz, G. C. The Optical Properties of Metal Nanoparticles: The Influence of Size, Shape, and Dielectric Environment. *J. Phys. Chem. B* **2003**, *107*, 668–677.
9. Murphy, C. J.; Sau, T. K.; Gole, A. M.; Orendorff, C. J.; Gao, Jx.; Gou, Lf.; Hunyadi, S. E.; Li, T. Anisotropic Metal Nanoparticles: Synthesis, Assembly, and Optical Applications. *J. Phys. Chem. B* **2005**, *109*, 13857–13870.
10. Mohamed, M. B.; Volkov, V.; Link, S.; El-Sayed, M. A. The 'Lightning' Gold Nanorods: Fluorescence Enhancement of Over a Million Compared to the Gold Metal. *Chem. Phys. Lett.* **2000**, *317*, 517–523.
11. Chou, C. H.; Chen, C. D.; Wang, C. R. C. Highly Efficient, Wavelength-Tunable, Gold Nanoparticle Based Optothermal Nanoconvertors. *J. Phys. Chem. B* **2005**, *109*, 11135–11138.
12. Eustis, S.; El-Sayed, M. Aspect Ratio Dependence of the Enhanced Fluorescence Intensity of Gold Nanorods: Experimental and Simulation Study. *J. Phys. Chem. B* **2005**, *109*, 16350–16356.
13. Wang, H. F.; Huff, T. B.; Zweifel, D. A.; He, W.; Low, P. S.; Wei, A.; Cheng, J.-X. *In Vitro* and *In Vivo* Two-Photon Luminescence Imaging of Single Gold Nanorods. *Proc. Natl. Acad. Sci. U.S.A.* **2005**, *102*, 15752–15756.
14. Durr, N. J.; Larson, T.; Smith, D. K.; Korgel, B. A.; Sokolov, K.; Ben-Yakar, A. Two-Photon Luminescence Imaging of Cancer Cells Using Molecularly Targeted Gold Nanorods. *Nano Lett.* **2007**, *7*, 941–945.
15. Link, S.; Wang, Z. L.; El-Sayed, M. A. How Does a Gold Nanorod Melt. *J. Phys. Chem. B* **2000**, *104*, 7867–7870.
16. Park, J.; Estrada, A.; Sharp, K.; Sang, K.; Schwartz, J. A.; Smith, D. K.; Coleman, C.; Payne, J. D.; Korgel, B. A.; Dunn, A. K.; *et al.* Two-Photon-Induced Photoluminescence Imaging of Tumors Using Near-Infrared Excited Gold Nanoshells. *Opt. Express* **2008**, *16*, 1590–1599.
17. Bouhelier, A.; Bachelot, R.; Lerondel, G.; Kostcheev, S.; Royer, P.; Wiederrecht, G. P. Surface Plasmon Characteristics of Tunable Photoluminescence in Single Gold Nanorods. *Phys. Rev. Lett.* **2005**, *95*, 267405.
18. Huff, T. B.; Hansen, M. N.; Zhao, Y.; Cheng, J.-X.; Wei, A. Controlling the Cellular Uptake of Gold Nanorods. *Langmuir* **2007**, *23*, 1596–1599.
19. Tong, L.; Zhao, Y.; Huff, T. B.; Hansen, M. N.; Wei, A.; Cheng, J.-X. Gold Nanorods Mediate Tumor Cell Death by Compromising Membrane Integrity. *Adv. Mater.* **2007**, *19*, 3136–3141.
20. Bickford, L.; Sun, J. T.; Fu, K.; Lewinski, N.; Nammalvar, V.; Chang, J.; Drezek, R. Enhanced Multi-spectral Imaging of Live Breast Cancer Cells Using Immunotargeted Gold Nanoshells and Two-Photon Excitation Microscopy. *Nanotechnology* **2008**, *19*, 315102.
21. Imura, K.; Nagahara, T.; Okamoto, H. Near-Field Two-Photon-Induced Photoluminescence from Single Gold Nanorods and Imaging of Plasmon Modes. *J. Phys. Chem. B* **2005**, *109*, 13214–13220.
22. Ni, W. H.; Kou, X. S.; Yang, Z.; Wang, J. F. Tailoring Longitudinal Surface Plasmon Wavelengths, Scattering and Absorption Cross Sections of Gold Nanorods. *ACS Nano* **2008**, *2*, 677–686.
23. Kou, X. S.; Zhang, S. Z.; Yang, Z.; Tsung, C.-K.; Stucky, G. D.; Sun, L. D.; Wang, J. F.; Yan, C. H. Glutathione- and Cysteine-Induced Transverse Overgrowth on Gold Nanorods. *J. Am. Chem. Soc.* **2007**, *129*, 6402–6404.
24. Tsung, C.-K.; Kou, X. S.; Shi, Q. H.; Zhang, J. P.; Yeung, M. H.; Wang, J. F.; Stucky, G. D. Selective Shortening of Single-Crystalline Gold Nanorods by Mild Oxidation. *J. Am. Chem. Soc.* **2006**, *128*, 5352–5353.
25. Sau, T. K.; Murphy, C. J. Room Temperature, High-Yield Synthesis of Multiple Shapes of Gold Nanoparticles in Aqueous Solution. *J. Am. Chem. Soc.* **2004**, *126*, 8648–8649.
26. Chen, H. J.; Kou, X. S.; Yang, Z.; Ni, W. H.; Wang, J. F. Shape- and Size-Dependent Refractive Index Sensitivity of Gold Nanoparticles. *Langmuir* **2008**, *24*, 5233–5237.
27. Kou, X. S.; Zhang, S. Z.; Tsung, C.-K.; Yeung, M. H.; Shi, Q. H.; Stucky, G. D.; Sun, L. D.; Wang, J. F.; Yan, C. H. Growth of Gold Nanorods and Bipyramids Using CTEAB Surfactant. *J. Phys. Chem. B* **2006**, *110*, 16377–16383.
28. Kou, X. S.; Ni, W. H.; Tsung, C.-K.; Chan, K.; Lin, H.-Q.; Stucky, G. D.; Wang, J. F. Growth of Gold Bipyramids with Improved Yield and Their Curvature-Directed Oxidation. *Small* **2007**, *3*, 2103–2113.
29. Demas, J. N.; Crosby, G. A. Measurement of Photoluminescence Quantum Yields. A Review. *J. Phys. Chem.* **1971**, *75*, 991–1024.
30. Lin, C.-A. J.; Yang, T.-Y.; Lee, C.-H.; Huang, S. H.; Sperling, R. A.; Zanella, M.; Li, J. K.; Shen, J.-L.; Wang, H.-H.; Yeh, H.-I.; Parak, W. J.; *et al.* Synthesis, Characterization, and Bioconjugation of Fluorescent Gold Nanoclusters toward Biological Labeling Applications. *ACS Nano* **2009**, *3*, 395–401.
31. Li, J. L.; Day, D.; Gu, M. Ultra-Low Energy Threshold for Cancer Photothermal Therapy Using Transferrin-Conjugated Gold Nanorods. *Adv. Mater.* **2008**, *20*, 3866–3871.
32. Huang, X. H.; El-Sayed, I. H.; Qian, W.; El-Sayed, M. A. Cancer Cell Imaging and Photothermal Therapy in the Near-Infrared Region by Using Gold Nanorods. *J. Am. Chem. Soc.* **2006**, *128*, 2115–2120.
33. Hauck, T. S.; Jennings, T. L.; Yatsenko, T.; Kumaradas, J. C.; Chan, W. C. W. Enhancing the Toxicity of Cancer Chemotherapeutics with Gold Nanorod Hyperthermia. *Adv. Mater.* **2008**, *20*, 3832–3838.
34. Skrabalak, S. E.; Chen, J. Y.; Sun, Y. G.; Lu, X. M.; Au, L; Cobley, C. M.; Xia, Y. N. Gold Nanocages: Synthesis, Properties, and Applications. *Acc. Chem. Res.* **2008**, *41*, 1587–1595.
35. Fischer, A.; Cremer, C.; Stelzer, E. H. K. Fluorescence of Coumarins and Xanthenes after Two-Photon Absorption with a Pulsed Titanium-Sapphire Laser. *Appl. Opt.* **1995**, *34*, 1989–2003.